SIMPLICITY, RIGOR AND RELEVANCE IN FLUID MECHANICS
F.J. Higuera, J. Jiménez and J.M. Vega (Eds.)

CHANGES IN PRESSURE AND WALL TENSION OCCURRING DURING THE ENLARGEMENT OF ABDOMINAL AORTIC ANEURYSMS

Anne-Virginie Salsac
Laboratory of Biomedical Flows
MAE Department
University of California, San Diego
La Jolla, CA 92093-0411, USA

Steven R. Sparks
Vascular Surgery
University of California, San Diego
San Diego, CA 92103-8403, USA

Juan C. Lasheras
Laboratory of Biomedical Flows
MAE Department
University of California, San Diego
La Jolla, CA 92093-0411, USA
Email: lasheras@mae.ucsd.edu
Web page:
http://www.mae.ucsd.edu

Abstract. The purpose of the study is to investigate the changes in velocity and pressure developing inside the sac of enlarging Abdominal Aortic Aneurysms (AAA).

A parametric in-vitro study of the pulsatile blood flow was conducted in laboratory models of AAAs by systematically varying the size of the aneurysm. The instantaneous pressure was measured over time in the parent vessel and at the location of maximum diameter inside the AAA. Simultaneously, the flow characteristics, corresponding to the physiological flow waveform inputted into the aneurysmal model, were quantified using Digital Particle Image Velocimetry (DPIV). Based on these results, a mechanism is proposed for the formation of the intra-luminal thrombus that is observed in 75% of later stage aneurysms.

Contrary to the prevailing intuition, we measure that, in the absence of endoluminal thrombus, the systolic pressure is lower in the aneurysm than in the parent vessel, for a certain range of aspect ratios (aneurysmal length to inlet diameter ratio) and dilatation parameters (maximum diameter to inlet diameter ratio). The pressure drop can be as high as 17%. However, this reduction in pressure does not automatically lead to a decrease in aneurysmal wall tension, since the latter also depends on other parameters, such as the local wall thickness and dimensions of the AAA. We show that, in spite of the pressure drop, the wall tension can increase by a factor of two, as the aneurysm enlarges. However, when an intra-luminal thrombus forms, the aneurysmal wall tension is shown to be reduced to near normal values.

Simultaneous measurement of the pressure and velocity field inside the AAA over time can be used to improve the prediction of the onset of endoluminal thrombus formation and the associated changes in the wall stresses acting on the aneurysmal sac.

Key words: abdominal aortic aneurysm, pulsatile flow, vascular mechanics, pressure, endoluminal thrombus

1. INTRODUCTION

The abdominal aorta is one of the sites of predilection for aneurysm formation. Abdominal aortic aneurysms (AAA) are a localized, abnormal dilatation of the infrarenal portion of the abdominal aorta, which occurs in 5 to 7 percent of the population over 60 years of age in Western countries [1,2]. The prevalence, which is higher for males and increases with age [3], was recently shown to be on a persistent rise for the last 20 years following a similar trend to other cardiovascular diseases [4]. The population at risk includes individuals over age 60, who smoke, have hypertension, diabetes, coronary heart diseases, high cholesterol and a family history of AAA [5-7]. About 75% of AAA are asymptomatic [8] and detection mainly occurs during unrelated radiological or surgical procedures. Once an aneurysm is formed, it enlarges due to a complex interplay between mechanical stimuli exerted by the pulsatile, unsteady blood flow and physiological changes occurring in the wall structure, mainly in the intima and media layers [9-12 among others]. As the abdominal aortic aneurysm (AAA) grows, the resultant morphological/structural changes in the arterial wall are coupled with changes in the hemodynamic stresses (local blood pressure and wall shear stresses). Morphological changes influence flow in the arterial segment and downstream of it. Inversely, changes in hemodynamic stresses can lead to the breakdown of the wall integrity by fostering thrombus formation, lipid deposition, calcification, etc [13-16]. Aneurysm rupture finally occurs when the wall tension exceeds the wall yield strength at any location on the wall [17].

The purpose of the study is to investigate the changes in velocity, pressure and in the corresponding wall tension inside the aneurysmal sac at progressive stages of enlargement of AAAs. The potential influence of disturbed flow conditions on the thrombus formation has long been recognized in AAA. Increasing experimental evidence indicates that low and oscillatory shear stresses promote proliferative, thrombotic, adhesive and inflammatory-mediated degenerative conditions throughout the arterial wall [18,19]. Although it has been suggested that the combined effect of the magnitude of shear stresses and the time interval during which the shear stresses act could be the determinant factor controlling this process [20], this mechanism has never been fully characterized. We discuss the mechanisms leading to the thrombus formation and the subsequent effects of the presence of a thrombus on the stresses acting on the aneurysm wall. This information will provide a much-needed tool for improving the assessment of the optimal time for surgical intervention.

2. MATERIALS AND METHODS

The experimental set-up is shown in Figure 1. The AAA models are placed in a flow loop, perfused with a glycerin/de-ionized water mixture of the same viscosity as blood. We hypothesize that for the application of interest, blood can be modelled as a Newtonian fluid, since the abdominal aorta is a large artery (diameter much larger than the critical value of 1 mm [21]).

Model number	D/d	L/d
1	2.1	2.9
2	1.3	2.9
3	1.9	2.9
4	2.4	2.9
5	2.9	5.7

Table 1. Geometric characteristics of the AAA models

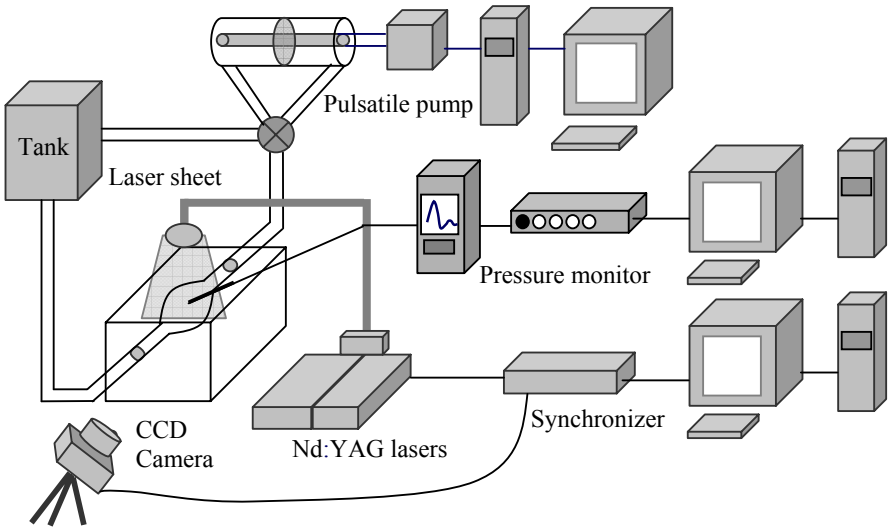

Figure 1. Experimental flow facility

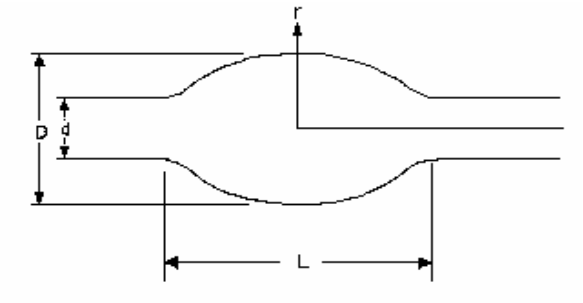

Figure 2. Shape and characteristic parameters of the AAA models

The AAA models consist of a symmetric, fusiform expansion, blown in a straight glass tube, as shown on Figure 2. These well-controlled axisymmetric shapes are characterized by 2 geometric parameters: the aspect ratio L/d (ratio of the aneurysm length to the inlet diameter) and the dilatation ratio D/d (ratio of the maximum diameter to the inlet diameter) (see Table 1). These parameters are systematically varied in our study in order to analyse the changes in the hemodynamic forces as the aneurysm grows. The effect of the vessel compliance was not considered in this study, since prior investigators [22-24] showed that, in general, the vessel compliance only slightly modifies the magnitude of the shear stresses but does not change the general characteristics of the flow, such as the pressure[†]. Furthermore, the effect of the wall distensibility is very small compared with the changes in anatomic dimensions studied here.

The unsteady flow is provided by a pulsatile, programmable pump. A rack-mounted piston is driven in a cylinder by a computed-controlled micro-stepping motor (Compumotor Corporation, Cupertino, CA). The piston divides the cylinder into 2 parts. A four-way spool valve (Numatics, Highlands, MI) is used to interchange the outlet and inlet pathways, when the piston reaches the end of its journey. This valve allows the pump to refill one side of the cylinder, while forcing fluid to exit from the other side. The pump

[†] The compliant nature of the arterial walls plays a critical role in the propagation of the pressure pulse and together with the architecture of the arterial tree, determines the shape of the pressure pulse (flow rate as a function of time) at each location. In our experiments, the models are rigid but the flow rate (pressure pulse) supplied to them by our system is identical to the input flow obtained from in-vivo measurements.

is programmed with flow patterns typical ofo the infrarenal aorta. However, no effort was made to simulate the secondary flow produced by the bifurcating renal arteries upstream of the AAA. The physiological flow waveform employed in this study is based on the results reported by Long et al. [25] (Figure 3), and corresponds to the case of a patient at rest, with a mean blood flow rate in the abdominal aorta of 1 liter/min and a period of cardiac cycle of 0.84 second (*i.e.* 72 pulses per minute). This flow condition corresponds to a peak Reynolds number $Re_p = 4Q_p/\pi d\nu = 2700$, a mean Reynolds number $Re_m = 4Q_m/\pi d\nu = 330$ and a Womersley number $\alpha = d/2(2\pi f/\nu)^{1/2} = 10.7$, where Q_p is the peak flow rate (at systole), Q_m the time-averaged flow rate, f the frequency and ν the kinematic viscosity.

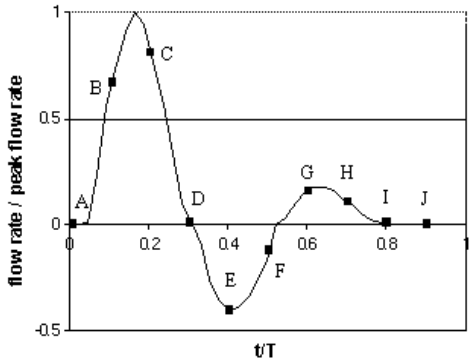

Figure 3. Flow waveform supplied to the AAA model and time location of the 10 measurements of the velocity field with the DPIV method

The instantaneous static pressure is measured over time with a Camino pressure probe (Olm intracranial pressure monitoring kit, Integra NeuroSciences^{TM}, Camino®), introduced at the wall at 2 locations: in the parent vessel, 2 cm upstream of the aneurysm, and inside the aneurysm at the location of maximum diameter. The probe's signal is fed to a pressure monitor (Camino V420) used to visualize the pressure signal, and to a digitising board (BNC 2090, National Instruments). The board is connected to a computer that is programmed to read and analyse the incoming signal.

The flow characteristics corresponding to the physiological flow waveform, programmed in the pump, are simultaneously quantified using Digital Particle Image Velocimetry (DPIV) (TSI Incorporated, St Paul, MN). This method enables the measurement of instantaneous velocity field inside the AAA along several cardiac cycles, at a sampling rate of 15 Hertz (the velocity field throughout the entire cross section of the AAA is measured every 1/15 s). The system is composed of two pulsed Nd:YAG lasers, a synchronizer, a CCD camera and a PC (Figure 1). The flow is seeded with 10 μm-diameter lycopodium particles (Carolina Biological Supply Company, Burlington, NC) that are illuminated, in one plane, by the pulsing laser sheet. The two lasers are fired at a time interval of 5-10 nanoseconds, illuminating the same cross-section of the aneurysm. The camera (630046 PIVCAM 10-30), 10^6 pixels, 8-bit resolution, records the position of the particles that scattered the light at each laser pulse. The digital image pairs are processed using the INSIGHT software, which calculates the instantaneous velocity field in the measuring plane. Other flow properties, such as the stress field $\tau = 0.5\mu(\partial u/\partial y+\partial v/\partial x)$, are then calculated from the measured velocity vectors $\vec{u} = (u,v)$, where x is the distance in the radial direction and y in the longitudinal one.

3. RESULTS

3.1 Characteristics of the flow inside the AAA and its changes during enlargement

The time evolution of the velocity field in a central axial plane of the aneurysm was measured using a DPIV system, with a sampling frequency of 15 measurements per second. The sequence of the velocity field that develops inside the aneurysm bulge is shown on Figure 4 for model 1 (Table 1). The 10 measurements composing the sequence are equally spaced in time and represent a full cardiac cycle (0.84s). The flow is from bottom to top in each figure. Time progresses along the cardiac cycle with the sequential labelling of the frames corresponding to that indicated in the cardiac waveform shown in Figure 3. These measurements clearly demonstrate not only that the behaviour of the pulsatile flow, inside the AAA, drastically differs from that of steady flows, but more importantly, that the flow inside the aneurysm is dominated by the formation of separated flow regions and by the development of a coherent vortex ring that traverses along the length of the AAA.

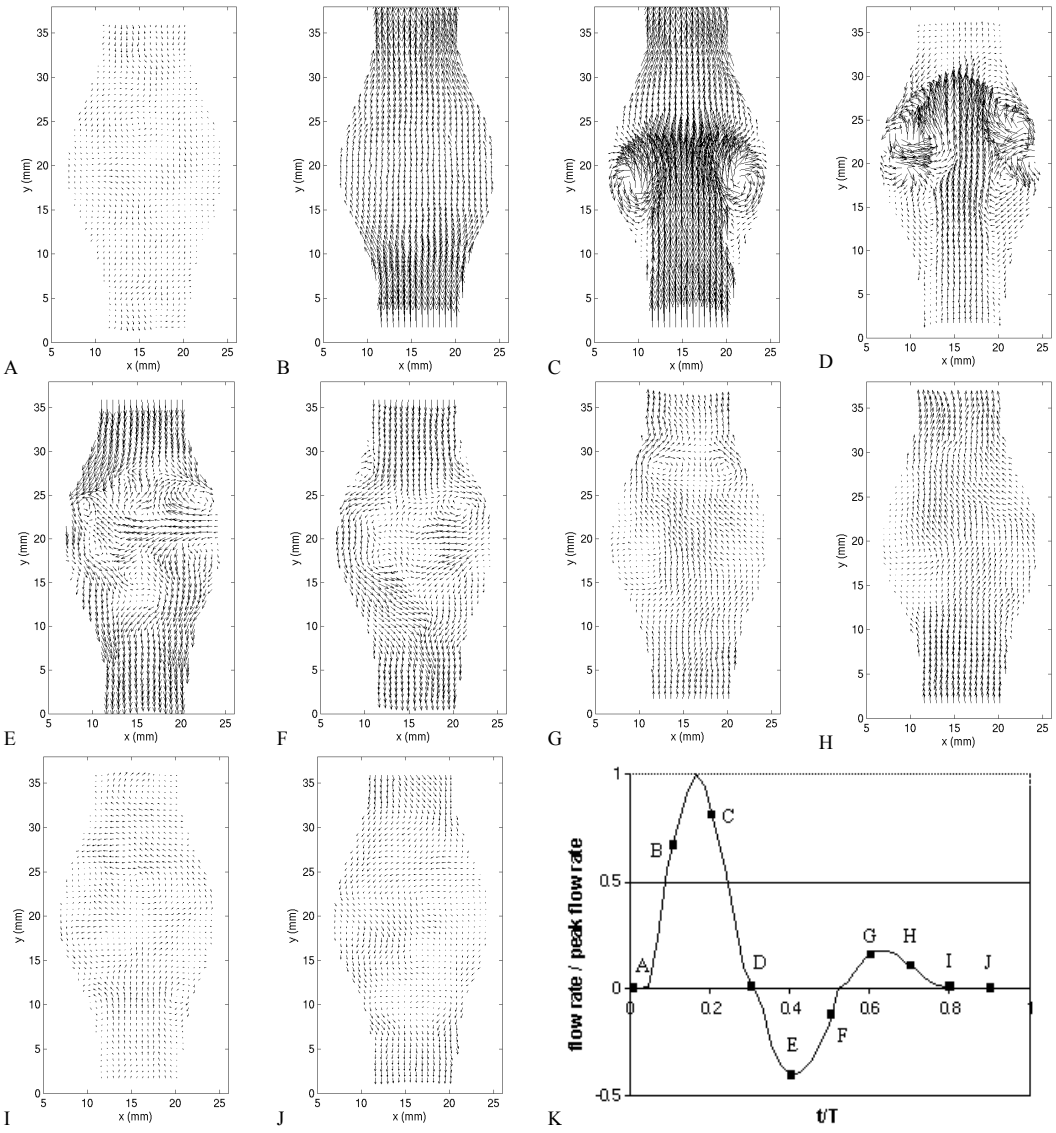

Figure 4. Time sequence of the velocity field measured in Model 1. The physiological flow waveform, shown in frame K, is based on the results reported by Long et al. [25]

These detailed velocity measurements reveal important features of the hemodynamics of AAA. For this particular geometry, the flow remains laminar and fully attached to the AAA walls during the entire acceleration portion of the systole (Figure 4 A-B). At the peak of the systole, the flow is still irrotational. At this point, the flow entering the AAA is nearly uniform across its entrance section and the thickness of the viscous layer on the vessel wall, which scales as d/α, is estimated to be about 1/10 of the diameter of the aorta. However, just after the initiation of the deceleration portion (Figure 4 C), the flow massively separates from the walls and a strong, coherent vortex ring is formed. During diastole, the vortex ring is observed travelling to the distal end of the AAA and internal shear layers appear across the entire length of the AAA. Regions of higher shear stresses are therefore created in the bulk of the blood flow. Another consequence of the formation of the vortex ring is the creation of large gradients in the wall shear stresses, as one moves from the proximal to the distal end of the AAA. As the vortex ring preceding this jet impinges on the distal neck, high wall shear stresses and spikes of pressure are generated locally, while the proximal half is dominated by a slow recirculating flow, exerting virtually no shear stress on the walls (Figure 4 D). At the peak diastole, the coherent shear layers and the preceding vortex ring break down, and a weak turbulent state is created inside the entire length of the AAA (Figure 4 E). During the resting portion of the cardiac cycle (Figure 4 F-J), the flow is observed to relaminarise as the turbulence created through the vortex breakdown slowly dissipates due to viscous stresses.

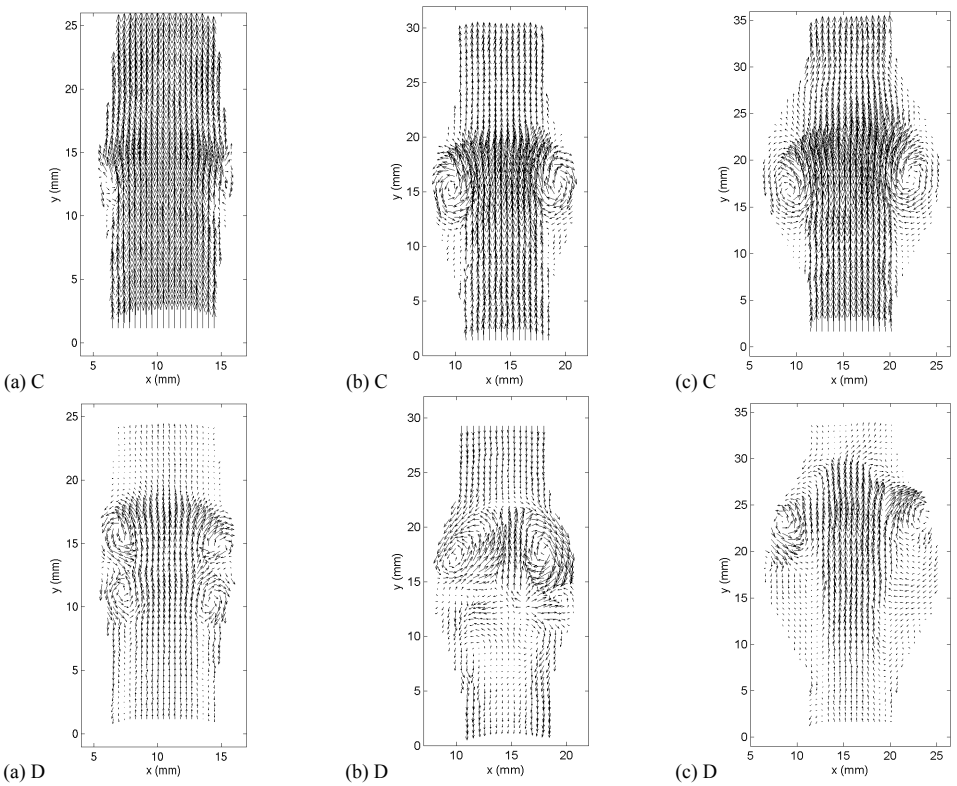

Figure 5. Velocity field measured after the peak systole at time steps C and D in (a) Model 2, (b) Model 3 and (c) Model 3.

The most important event that characterizes flow in an aneurysm is the flow separation in the deceleration phase of the cardiac cycle. Figure 5 compares flow separation inside the AAA at three progressive stages in the enlargement. The flow field is respectively shown for Models 2, 3 and 4 at the 2 critical time steps (C and D) during which

flow separation occurs (Table 1). One can observe the changes in the velocity field related to the aneurysm growth. When comparing frame C in the 3 figures, a distinct increase in the size of the vortex can be seen with increasing aneurysmal diameter, which leads to a proportional increase in the vortex strength. The size of the flow recirculation region increases simultaneously, subjecting a larger portion of the wall to very low wall shear stresses, when the distal part of the wall is subjected to large wall shear stresses, around the point of vortex impingement. The wider the aneurysm, the larger the wall shear stress gradients are likely to be along the aneurysm wall.

Although the onset of separation is a function of the two geometrical parameters, D/d and L/d, we have observed that it occurs for dilatation ratios as small as of 1.3 (model 2). This is a consequence of the large deceleration characteristic of the diastolic flow in the abdominal aorta. Thus, separation should occur even in incipient aneurysms[‡].

3.2 Pressure measurements

The pressure was measured in 4 significant AAA models in the parent vessel and at the location of maximum diameter in the aneurysm. Figure 6 shows the pressure waveform non-dimensionalised with the systolic pressure for models 2 and 3. Due to the lack of compliance of the downstream reservoir, the shape of the pressure waveform measured in our experiment does not correspond to what is typically measured in vivo in the abdominal aorta. In this experiment, only the abdominal aorta was modelled and not the whole arterial system. Instead of inputting a pressure waveform induced by the heart and letting this pressure wave evolve as a function of the whole arterial compliance and geometry, we input directly the flow waveform at the entrance of the abdominal aorta, as measured in vivo. This technique results in a waveform somewhat different to the physiological one, but it allows us to measure qualitatively the possible changes in pressure, as a result of the growth of the AAA.

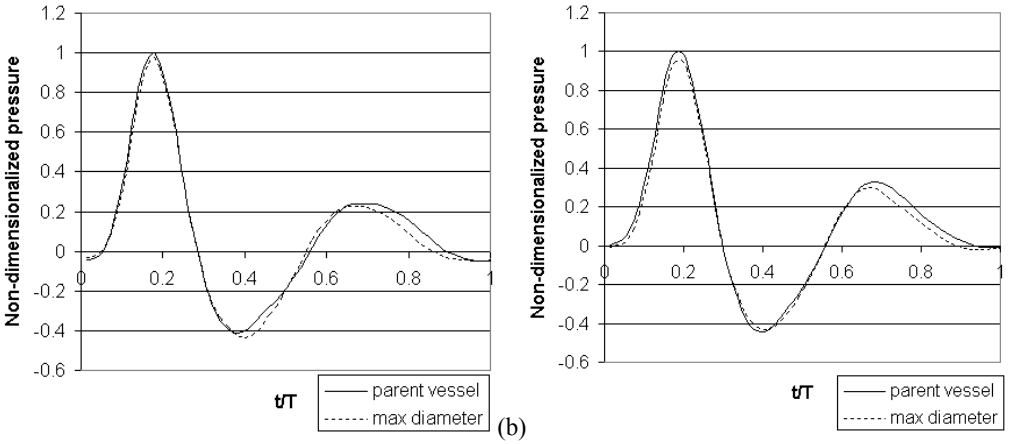

Figure 6. Comparison of the pressure measurement in the parent vessel and at the location of maximum diameter for Model 1 (a) and Model 2 (b). The pressure has been non-dimensionalised with the systolic pressure in each case.

It was measured that, inside the aneurysm, the systolic pressure decreased slightly (~ - 3%). This decrease in systolic pressure in the AAA was observed consistently regardless of its size. We found that the pressure drop actually increased as the aneurysm enlarged, to reach 17% in Model 5. A summary of the results of the pressure drops is given in Table 2.

[‡] Clinically, a vessel dilatation is considered an aneurysm when $D/d \geq 1.5$.

Model number	% of decrease in systolic pressure
2	2.5%
3	3.4%
4	7%
5	17%

Table 2. Percentage of decrease in the systolic pressure in the AAA compared with the one in the parent vessel.

3.3 Endoluminal thrombus formation

The velocity measurements show that the hemodynamic wall stresses, *i.e.* the distribution of pressure and shear stresses on the aneurysm's walls, depend on the geometric parameters of the aneurysm, L/d and D/d. The important question to be elucidated is the role that the disturbed stress conditions could play on the formation of an endoluminal thrombus in an AAA.

The DPIV measurements show that the flow inside the AAA massively detaches during diastole forming large regions of slowly recirculating regions close to the walls. The formation and size of the region of flow recirculation was found to be enhanced as the size of the AAA was increased. The flow separation also led to the formation of internal shear layers, characterized by higher shear stresses than measured in a healthy abdominal aorta. This suggests that the circulating blood cells are exposed to different patterns of stresses when entering the AAA.

In order to quantify the time history of the shear stresses acting on individual circulating cells, we have developed at the UCSD laboratory of Biomedical Flows a code that computes the trajectory of the blood cells inside the aneurysm. We follow the Lagrangian evolution of the cells, by computing, at each time step, the location where the cell travels to, based on the DPIV phase-averaged velocity measurements performed along the full cardiac cycle.

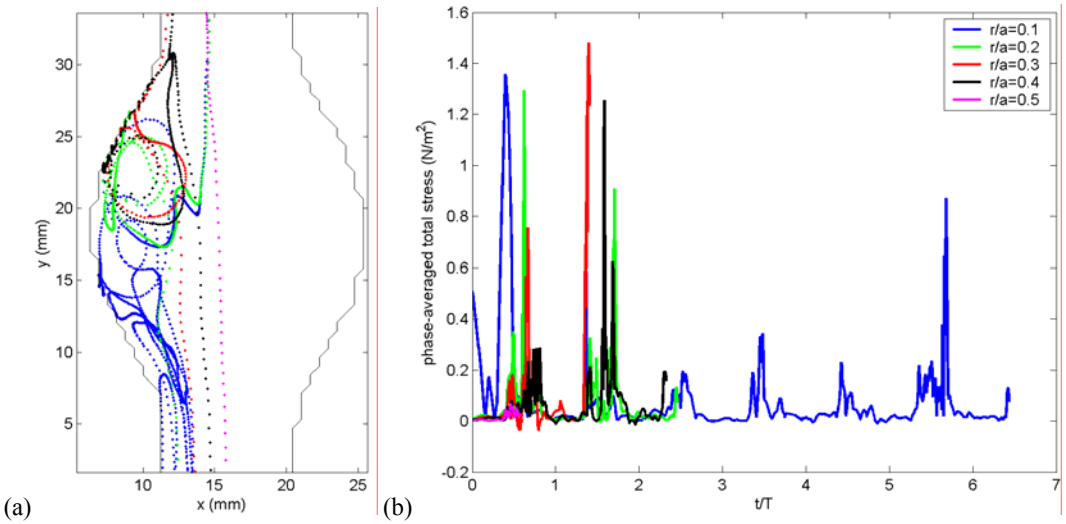

Figure 7. Comparison of the time history of shear stresses experienced by a blood cell entering Model 5 at a distance x/d = 0.1, 0.2, 0.3, 0.4 or 0.5 from the wall.

Figure 7 shows the computed trajectories of the blood cells (a) and the time evolution of the shear stresses (b) for 5 representative cells entering the aneurysm at different locations from the wall. The stresses plotted in Figure 7(b) are the Lagrangian stresses the

cells experience when transported inside the AAA. They have been phase-averaged over 6 cardiac cycles to take into account the cycle-to-cycle variations resulting from the weak turbulence at the end of each cycle. In these computations, the flow inside the AAA has been assumed to be symmetric and the cell trajectories confined to the symmetry plane. Measurements of the three-dimensional, streamwise vortices formed in the internal shear layers have shown that their induced velocity is small compared to the one measured in the symmetry plane. Thus, in a first approximation, the symmetry assumption will give a first order estimate of the values of the stresses. However, the time history of the stresses could be somewhat different than the ones computed in this study. The three-dimensional effects are discussed elsewhere [26].

Analysis of the trajectories show that the blood cells entering the AAA near the arterial walls are subjected to higher levels of shear stresses in the internal shear layer, while they are later entrained in the regions of stasis, where they remain in the vicinity of the wall. The resident time of these cells has been found to increase up to 7 cardiac cycle (Figure 7 (b)). The blood cells entering closer to the centre of the vessel are entrained by the vortex ring towards the distal part of the arterial wall. The cells stay close the wall until the next systolic acceleration. Therefore, flows inside aneurysms have the peculiarity of bringing blood cells near the wall, enhancing their chance of adhering to it. Wall adhesion will occur in areas where endothelial cells are activated.

In a healthy vessel, the only cells that experience a non-zero shear stress are the ones travelling in a region close to the wall, which represents about one third of all cells. On the contrary, *all* the cells are subjected to some degree of shear stress in an aneurysm. Moreover the amplitude of the stresses acting on the cells has been measured to be 3 times higher with strong fluctuations over time. The stresses peak as the blood cells approach the wall during systole or the shear layer during diastole.

4. DISCUSSION

4.1 Luminal pressure and wall tension

The observed decrease in systolic pressure is not obvious and may, at first sight, appear counterintuitive to the clinical community. However, it is a clear consequence of the behaviour of the unsteady flow in the cavity and it can be predicted using the unsteady form of the Bernoulli's equation

$$\rho\frac{\partial\vec{u}}{\partial t}+\nabla\left(\frac{1}{2}\rho\vec{u}^{\,2}+p+\rho gz\right)=\vec{u}\times\vec{\omega}+\nu\nabla^{2}\vec{u} \qquad (1)$$

If the flow were steady, equation (1) would reduce to the familiar form of the Bernoulli's equation, which states that $\frac{1}{2}\rho\vec{u}^{\,2}+p+\rho gz$ is constant along a streamline. This would imply that the pressure inside the AAA increases as a consequence of the decrease in the velocity, which occurs by virtue of the mass conservation equation in a diverging wall configuration. However, in our case the flow entering the AAA is pulsatile and an additional contribution to the pressure gradient arises from the acceleration/deceleration term present on the left-hand side of equation (1), $\rho\frac{\partial\vec{u}}{\partial t}$.

In the case of irrotational flows (as observed on Figure 4 B), the unsteady Bernoulli's equation further simplifies to the form:

$$\rho \frac{\partial v}{\partial t} + \frac{\partial p}{\partial y} + \frac{\partial}{\partial y}\left(\frac{1}{2}\rho \vec{u}^2\right) = 0 \qquad (2)$$

In the divergent section, the change in kinetic energy is negative, while the temporal acceleration is positive. The unsteady acceleration term is therefore the cause of the decrease in systolic pressure measured inside the AAA. This shows that, as long as the flow remains attached during systole, the temporal acceleration term is slightly larger in amplitude than the change in kinetic energy, so the systolic pressure inside the AAA is smaller than the one measured upstream in the parent vessel.

The internal pressure acting on the artery wall produces a circumferential tension through the wall. This tension that is exerted in a direction tangential to the artery wall and perpendicular to a longitudinal section tends to tear the vessel apart. Let us first consider the case of an AAA before the formation of an endoluminal thrombus. In a first order of magnitude approximation, the maximum value of the wall tension can be estimated by the Law of LaPlace (a detail calculation would require the use of a finite element model, based on the knowledge of the local wall thickness and of the material properties of the wall). Approximating locally the shape of the AAA to a cylinder with a finite wall thickness, this law relates the averaged peak circumferential tension across the wall σ_θ to the systolic pressure p_s and to the vessel geometry:

$$\sigma_\theta = \frac{p_s r}{\delta} \qquad (3)$$

where r is the local radius of the vessel and δ the wall thickness. Equation (3) shows that, if p_s remains identical or even if it decreases slightly inside the AAA, the extensional tension may increase due to changes in r and δ. As the AAA enlarges, the wall thickness tends to increase slightly but the radius increases substantially resulting in a net increase in σ_θ. In the case of model 5 for example, the systolic pressure inside the AAA decreases by 17%, the wall thickness increases by 16.7% [27] while the aneurysmal radius triples, which leads to an increase of the wall tension by more than 200%!

4.2 Endoluminal thrombus

As the AAA enlarges, the platelets and red blood cells are locally subjected to higher levels of shear stresses. In these regions, the cells are likely to get moderately activated and aggregate to one another. Without any further stimulation, the aggregates were found to dissolve very quickly [28]. However this moderate state of activation and aggregation can then be reinforced by the length of time spent in regions of low stresses, which are known to foster aggregation [29]. The resident times in the flow recirculating regions was calculated to be of the order of several cardiac cycles.

The endothelial cells lining the vessels also react to the changes in mechanical stimuli in the AAA. They have been shown to get activated both in regions of large gradients of wall shear stresses (as in the distal neck of the AAA) [30-32] and in regions of low and oscillating wall shear stresses (as in the proximal neck of the AAA) [19, 33]. The particle tracking showed that the blood cells preferentially come very close to the wall in these 2 distinct regions. The activated state of the endothelial cells will therefore allow for the wall adhesion of the already partially aggregated blood cells. The combination of moderate cell-activation in high stress regions, consecutive entrainment in regions of low stresses, long resident times and the activation of the endothelium cells due to low wall shear stresses creates the optimal cell-adhesive and inflammatory-mediated degenerative conditions that leads to the formation of the endoluminal throm-

bus. The thrombus is postulated to play an important role on the pathogenesis and progressive enlargement of AAAs.

When the thrombus is formed and an endoluminal channel is created, the extensional tension on the AAA walls is drastically reduced by a factor, which can be estimated as the ratio between the endoluminal channel surface to the AAA surface [34,35]. The thrombus transmits the pressure to the wall, but does not contribute to the mechanical strength of the wall. Estimates obtained from three-dimensional volume rendering of CT scans performed in several of San Diego VA Hospital patients with large AAA shows that this ratio is of the order of 2. Thus, it appears that, when the endoluminar thrombus forms, it may reduce the wall extensional tension in the AAA to near normal values, and in this regard increase the structural integrity of the vessel. However, this gain in structural strength is at the cost of a drastic reduction in oxygen diffusion to the medial layer [36,37], the disappearance of all endothelium-derived regulatory processes and the onset of inflammatory-mediated degenerative conditions throughout the arterial wall and within the thrombus itself [38-40]. All of these factors are known to contribute to the further deterioration of the median layer, which is key to the structural strength of the wall and to the continued or even accelerated enlargement of the AAA [41].

5. CONCLUSION

Measurements conducted in rigid symmetric AAA models have shown that, for the large diastolic deceleration, characteristic of abdominal aortic flows, flow separation occurs at very early stages during the AAA formation ($D/d \geq 1.3$). The flow separation, the associated formation of internal shear layers and the recirculating regions provide the optimal flow conditions for the formation of an intraluminal thrombus.

We have shown that, contrary to what is believed, the systolic pressure remains constant or decreases slightly as the AAA enlarges. This pressure decrease, however, does not lead to a reduction in wall tension, which in the absence of endoluminal thrombus may increase up to a two fold. However, the presence of thrombus may lead to a re-establishment of the wall tension to near-normal values.

These measurements can be further combined with the computation of the wall tension by finite element methods, to provide a guideline to establish an improved criterion predicting the AAA rupture, with or without the presence of an intraluminal thrombus, as a function of the geometrical parameters and hemodynamic conditions of the patient.

REFERENCES

[1] K. Singh, K.H. Bønaa, B.K. Jacobson, L. Bjørk and S. Solberg. Prevalence of and risk factors for abdominal aortic aneurysms in a population-based study. *Am. J. Epidemiol.* **154**, 236--244 (2001).

[2] M. Lawrence-Brown, P.A. Norman, K. Jamrozik, J.B. Semmens, N.J. Donnelly, C. Spencer and T. Raywin. Initial results of ultrasound screening for aneurysm of the abdominal aorta in Western Australia: relevance for endoluminal treatment of aneurysm disease. *Cardiovasc Surg.* **9**, 234--240 (2001).

[3] J. Collin. The epidemiology of abdominal aortic aneurysm. *British Journal of Hospital Medicine*. **40**, 64--67 (1988).

[4] V.A. Best, J.F. Price and F.G.R. Fowkes. Persistent increase in the incidence of abdominal aortic aneurysm in Scotland, 1981-2000. *Brit. J. Surg.* **90**, 1510--1515 (2003).

[5] J.M. Reilly, M.D. Tilson. Incidence and etiology of abdominal aortic aneurysms. *Abdominal aortic aneurysms*. Saunders, 689--898 (1989).

[6] F. Valdes, N. Sepulveda, A. Kramer, R. Mertens, M. Bergoeing, L. Marine, M. Alcarte, J.P. Carbonell, L. Burgos, M. Lagos, M. Fava, C. Wong and J. Vergara, "Frequency of abdominal aortic aneurysms in adult population with known risk factors", *Rev. Med. Chil.* **131**, 741--747 (2003).

[7] H. Bengtsson, B. Sonesson and D. Bergqvist. Incidence and prevalence of abdominal aortic aneurysms, estimated by necropsy studies and population screening by ultrasound. *The abdominal aortic aneurysm: genetics, pathophysiology, and molecular biology*. N.Y. New York Academy of Sciences, (1996).

[8] A.V. Pokrovskii, V.N. Dan, A.M. Zlatovchen and S.A. Il'in. The impact of cardiac status and arterial hypertension on the results of surgical treatment of patients over 70 years with abdominal aortic aneurysms. *Angiol. Sosud. Khir.* **9**, 71--76 (2003).

[9] T. Fukushima, T. Matsuzawa and T. Homma. Visualization and finite element analysis of pulsatile flow in models of the abdominal aortic aneurysm. *Biorheology*. **26**. 109--130 (1989).

[10] C.A. Taylor, T.J.R. Hughes and C.K. Zarins. Finite elements modeling of three-dimensional pulsatile flow in the abdominal aorta: relevance to atherosclerosis. *Ann. Biomed. Eng.* **26**, 975--987 (1998).

[11] C.J. Egelhoff, R.S. Budwig, D.F. Elger, T.A. Khraishi and K.H. Johansen. Model studies of the flow in abdominal aortic aneurysms during resting and exercise conditions. *J. Biomech.* **32**, 1319--1329 (1999).

[12] A.-V. Salsac, S.R. Sparks and J.C. Lasheras. Hemodynamic changes occurring during the progressive enlargement of abdominal aortic aneurysms. *Ann. Vasc. Surg.* **18**, 14--21 (2004).

[13] E. Di Martino, S. Mantero, F. Inzoli, G. Melissano, D. Astore, R. Chiesa and R. Fumero. Biomechanics of abdominal aortic aneurysm in the presence of endoluminal thrombus: experimental characterization and structure static computational analysis. *Eur. J. Vasc. Endovasc. Surg.* **15**, 290--299 (1998).

[14] D. Bluestein, L. Niu, R.T. Schoephoerster and M.K. Dewanjee. Steady flow in an aneurysm model: correlation between fluid dynamics and blood platelet deposition. *J. Biomech. Eng.* **118**, 280--286 (1996).

[15] F.J. Miller, W. J. Sharp, X. Fang, L.W. Oberley, T.D. Oberley and N.L. Weintraub. Oxidative stress in human abdominal aortic aneurysms: a potential mediator of aneurysmal remodeling. *Arterioscler. Thromb. Vasc. Biol.* **22**, 560--565 (2002).

[16] E. Papagrigorakis, D. Iliopoulos, P.J. Asimacopoulos, H.J. Safi, D.J. Weilbaecher, K.G. Ghazzaly, M.L. Nava, J.W. Gaubatz and J.D. Morrisett. Lipoprotein (a) in plasma, arterial wall, and thrombus from patients with aortic aneurysm. *Clin. Genet.* **52**, 262--271 (1997).

[17] J.L. Cronenwett. Variables that affect the expansion rate and rupture of abdominal aortic aneurysms. *The abdominal aortic aneurysm: genetics, pathophysiology, and molecular biology*. N.Y. New York Academy of Sciences, (1996).

[18] C.G. Caro, J.M. Fitz-Gerald and R.C. Schroter. Atheroma and arterial wall shear, observations, correlation and proposal of a shear dependant mass transfer mechanism for atherogenesis. *Proc. R Soc. London B.* **177**, 109--159 (1971).

[19] J.E. Moore, C. Xu, S. Glagov, C.K. Zarins and D.N. Ku. Fluid wall shear stress measurements in a model of the human abdominal aorta: oscillatory behavior and relationship to atherosclerosis. *Atherosclerosis.* **110**, 225--240 (1994).

[20] D. Bluestein, E. Rambod and M. Gharib. Vortex shedding as a mechanism for free emboli formation in mechanical heart valves. *J. Biomech. Eng.* **122**, 125--134 (2000).

[21] W.W. Nichols and M.F. O'Rourke. *McDonald's blood flow in arteries: theoretic, experimental and clinical principles.* Lea & Febiger, (1990).

[22] D.D. Duncan, C.B. Bargeron, S.E. Borchardt, O.J. Geters, S.A. Gearhart, F.F. Mark and M.H. Friedman. The effect of compliance on wall shear in casts of a human aortic bifurcation. *J. Biomech. Eng.* **112**, 183--188 (1990).

[23] H.J. Steiger, A. Poll, D. Liepsch and H.J. Reulen. Haemodynamic stress in lateral saccular aneuyrsms. An experimental study. *Acta Neurochir.* **86**, 98--105 (1987).

[24] H.J. Steiger, A. Poll, D.W. Liepsch and H.J. Reulen. Haemodynamic stress in terminal aneurysms. *Acta Neurochir*. **93**, 18--23 (1988).

[25] Q. Long, X.Y. Xu, M. Bourne and T.M. Griffith. Numerical study of blood flow in an anatomically realistic aorto-iliac bifurcation generated from MRI data. *Magn. Reson. Med.* **43**, 565--576 (2000).

[26] A.-V. Salsac. PhD thesis. University of California, San Diego (2004).

[27] A. Ghorpade and B.T. Baxter. Biochemistry and molecular regulation of matrix macromolecules in abdominal aortic aneurysms. *The abdominal aortic aneurysm: genetics, pathophysiology, and molecular biology*. N.Y. New York Academy of Sciences, (1996).

[28] J. N. Zhang, A.L. Bergeron, Q. Yu, C. Sun, L.V. McIntire, J.A. López and J.F. Dong. Platelet aggregation and activation under complex patterns of shear stress. *Thromb. Haemost.* **88**, 817--821 (2002).

[29] B.R. Alveriadou, J.L. Moake, N.A. Turner, Z.M. Ruggeri, B.J. Folie, M.D. Phillips, A.B. Schreiber, M.E. Hrinda and L.V. McIntire. Real-time analysis of shear dependent thombus formation and its blockade by inhibitors of Van Wilebrand factors binding to platelets. *Blood*. **81**, 1263--1276 (1993).

[30] N. DePaola, M. Gimbrone, P. Davies and C. Dewey. Vascular endothelium responds to fluid shear stress gradients. *Arterioscler. Thromb.* **12**, 1254--1257 (1992).

[31] Y. Tardy, N. Resnick, T. Nagel, M. Gimbrone and C. Dewey. Shear stress gradients remodel endothelial monolayer in vitro via a cell proliferation-migration-loss cycle. *Arterioscler. Thromb. Vasc. Biol.* **17**, 3102--3106 (1997).

[32] T. Nagel, N. Resnick, C.F. Dewey and M.A. Gimbrone. Vascular endothelial cells respond to spatial gradients in fluid shear stress by enhanced activation of transcription factors. *Arterioscler. Thromb. Vasc. Biol.* **19**, 1825--1834 (1999).

[33] G. Helmlinger, B.C. Berk and R.M. Nerem. Calcium responses of endothelial cell monolayers subjected to pulsatile and steady laminar flow differ. *Am. J. Physiol.* **269**, C367--C375 (1995).

[34] D.H. Wang, M. Makaroun, M.W. Webster and D.A. Vorp. Mechanical properties and microstructure of intraluminal thrombus from abdominal aortic aneurysm. *J. Biomech. Eng.* **123**, 536--539 (2002).

[35] W.R. Mower, W.J. Quinones and S.S. Gambhir. Effect of intraluminal thrombus on abdominal aortic aneurysm wall stress. *J. Vasc. Surg.* **26,** 602--608 (1997).

[36] D.A. Vorp, D.H.J. Wang, M.W. Webster and W.J. Federspiel. Effect of intraluminal thrombus thickness and bulge diameter on the oxygen diffusion in abdominal aortic aneurysm. *J. Biomech. Eng.* **120**, 579--583 (1998).

[37] D.A. Vorp, P.C. Lee, D.H. Wang, M.S. Makaroun, E.M. Nemoto, S. Ogawa and M.W. Webster. Association of intraluminal thrombus in abdominal aortic aneurysm with local hypoxia and wall weakening. *J.Vasc. Surg.* **34**, 291--299 (2001).

[38] M. Gacko and S. Głowiński. Activities of proteases in parietal thrombus of aortic aneurysm. *Clin. Chim. Acta.* **271**, 171--177 (1998).

[39] V. Fontaine, M.-P. Jacob, P. Rossignol, D. Plissonnier, E. Angles-Cano and J.-B. Michel. Involvement of the mural thrombus as a site of protease release and activation in human aortic aneurysms. *Am. J. Pathol.* **161**, 1701--1710 (2002).

[40] J. Satta, E. Laara and T. Juvonen. Intraluminal thrombis predicts rupture of an abdominal aortic aneurysm. *J. Vasc. Surg.* **23**, 737--739 (1996).

[41] M. Kazi, J. Thyberg, P. Religa, J. Roy, P. Eriksson, U. Hedin and J. Swedenborg. Influence of intraluminal thrombus on structural and cellular composition of abdominal aortic aneurysm wall. *J. Vasc. Surg.* **38**, 1283--1292 (2003).